APPENDIX 3C: Internal Accuracy and Precision of Particulate Data

3C.1 Definitions

In this section we will express the uncertainty as either fractional uncertainty, $f(x)$, or absolute uncertainty, $\sigma(x)$, depending on which form is appropriate. If one form is expected to be constant, we will use that form. For example, the uncertainty in volume for a given sampler will be a constant fraction, so we will use the fractional form for it. The analytical uncertainty for mass is independent of the magnitude of the mass, so the absolute form is appropriate. In all cases, the fractional and absolute uncertainties are related by the value of the variable.

For a given variable, there may be an artifact due to one of several sources: conversion of gas to particles in the filter; contamination of the filter material or contamination introduced during analysis and/or transport, and; contamination introduced during analysis. We will denote this artifact by the traditional B, with the proviso that it is not necessarily the blank. (For example, this B is not the tare mass of the clean filter.) If M is the measured mass of the variable and V is the volume of air, then the concentration is given by

$$C = (M - B)/V.$$

The uncertainty in concentration is given by

$$\sigma^2(c) = c^2 f^2(V) + \sigma^2(M)/V^2 + \sigma^2(B)/V^2$$

The fractional uncertainty in the volume is equal to the fractional uncertainty in the flow rate and is a constant, at least within certain limits of flow rate. In general, $\sigma(B)$ is also a constant for a given variable, although it might vary with site, season, or analytical condition. For some analytical methods B and $\sigma(B)$ may be zero, as with the x-ray methods and PESA.

However, the analytical uncertainty, $\sigma(M)$, may have several possible forms. It may be constant, independent of the magnitude of M, as in gravimetric analysis and the TOR carbon analysis. It may be proportional to M, so that $f(M)$ is constant, as in the IC analysis of the IMPROVE samples. In the third case, $\sigma(M)$ depends on M and on other factors of the analysis, such as counting statistics, in some complicated manner. For the x-ray methods and PESA, $\sigma(M)$ must be calculated by the analytical codes at the time of analysis.

We will define the minimum detectable limit (mdl) in one of two ways. For spectral methods (x-ray, PESA), the mdl is the concentration that would result if the number of counts for the

defining peak were equal to 3.29 times the square root of the number of counts in the background under the peak. If σ is the uncertainty for this case where the filter is clean, the mdl is 2.3σ. For other analytical methods, we will define the mdl by

$$mdl = 2\sigma,$$

where σ is the uncertainty when the filter is clean, or the measured value equals the artifact value. The mdl in this second case could also be called the minimum quantifiable limit. For these methods, σ is either the uncertainty in the artifact, $\sigma(B)$, or the quadratic sum of the artifactual and analytical uncertainties. The analytical uncertainty must be included in the mdl when it is nonzero for a clean sample, such as in gravimetric and TOR analyses.

3C.2 IMPROVE Sampler

Precision and Accuracy of Air Volume

The volume is calculated from the average flow rate and sample duration using the relationship

$$Volume(m^3) = flow\ rate(l/min) * duration(hours) * 60/1000.$$

Since the fractional uncertainty in flow rate is much larger than that in duration, the uncertainty in volume depends predominately on the uncertainty in flow rate. That is, the fractional uncertainty in volume equals the fractional uncertainty in flow rate.

The IMPROVE flow rate is measured by an internal orifice-meter system that measures the pressure drop across the inlet and cyclone using a magnehelic gauge. This internal system was calibrated at the site using an external orifice-meter system. The external meter was in turn calibrated at Davis both before and after the study using a spirometer; the readings were corrected for temperature and pressure of the WHITEX site using standard equations. The flow rate Q is obtained from the reading ΔP on the internal magnehelic using the empirical equation

$$Q = a(\Delta P)^b,$$

where a is around 35 l/min and b is around 0.44.

The volume calculation depends on the average flow rate over the sampling period, as controlled by the critical orifice. The flow rate will change if the pressure drop across the filter or the temperature of air at the critical orifice changes. Increasing the pressure drop across the filter will cause a slight decrease in flow rate; this is the justification for measuring flow rates before and after sampling. The temperature variation for the critical orifice equation also goes as the square root of the temperature. Thus, the average flow rate is given by

$$\text{average } Q = \frac{a}{2}[(\Delta P_1)^b + (\Delta P_2)^b](T_m/T_c)^{1/2},$$

where ΔP_1 and ΔP_2 are the initial and final readings and T_m is the average temperature over the collection period. Note that the average flow rate does not depend on the temperatures at the times of measurement. The average temperature was calculated from the meteorological measurements made at the site.

The precision and accuracy of the IMPROVE flow rate can be estimated from the independent audit conducted by C. Lalane of ERT during the period from January 8 to 15. The audit device was a standard orifice meter, with a water manometer used to measure the pressure drop across a calibrated orifice. The system was calibrated at the ERT laboratory and corrected for temperature

and pressure. The accuracy of the IMPROVE system can be estimated from the average ratio of the flow rates of the IMPROVE internal system to the audit system. The IMPROVE flow rates were based on readings of Lalane at the time of the audit. The precision can be estimated from the standard deviation of the ratios.

The audit was conducted during the first week of the WHITEX study, before the UCD field engineer validated the setup of all of the samplers. In two cases the samplers had been setup incorrectly. At Monticello, the data is for the second audit, made after the sampler was correctly assembled. The critical orifice in Mexican Hat module M was missing at the time of the audit; accordingly no audit value exists for this module. Samples collected before the correct setup were excluded from the data base.

The results of the audit for all nine sites with IMPROVE samplers are shown in Table 3C.1. In 44 of the 45 cases, the flow rates were between 18 and 22 l/min. For these 44 cases, the average ratio of internal/audit was 1.017±0.031. In the 45th case, Hopi Point module B, both internal and audit values were well below 18 l/min and the agreement was poor. The reason for the low flow rate was that the impregnated filter for this particular period had an extremely large pressure drop. The most likely reason for the disagreement is that either the Hopi Point module B or the audit device was not calibrated properly for this abnormally low flow rate. The Hopi Point situation was recreated at UCD after the study: the system was calibrated in the region of 17–25 l/min and the pressure drop increased to reduce the flow rate to 10 l/min. In this case, the flow rate measured on the internal system agreed with a mass flow meter and the spirometer to within 3%. This indicates that the calibration curve for the internal system is linear down to 10 l/min, but does not prove that the internal measurements were correct. However,there is no reason to assume that the internal and audit devices would disagree for a normal flow rate. Thus, this point was eliminated in the precision estimate. If the calibration were wrong, only a small fraction of the module B samples would have incorrect volumes.

In order to quantify the precision and accuracy of the sampler flow rates, the audit device should be more accurate and precise than the sampler device. Because the IMPROVE internal flow rate measurement system is based on the same orifice-meter principle as the audit device, this criterion is not met. In order to quantify the precision of the IMPROVE sampler, it is necessary to make an estimate of the precision of the audit device. One option is to use the nominal accuracy stated by ERT for the precision, namely 3%; in this case, the precision of the IMPROVE sampler flow rate is less than 1%. A second option is to assume that the precision of the audit device is negligibly small; in this case, the IMPROVE precision is 3%. The third option is to assume that the precisions of both audit and internal systems are equal; in this case, both systems have a precision of 2%. Since the volume calculation is based on two readings of the flow rate, the precision of the volume is equal to the flow rate precision divided by 1.414. Thus,the volume precision based on the audit is between 0.6% and 2.2%. For the uncertainties in the data base,we have used a conservative estimate, setting the volume precision to 3%, using a lower estimate would not have a major effect on the quoted uncertainties.

In order to verify that this precision estimate is reasonable, we can calculate the precision of the measurement from the reading of the magnehelic. Since flow rate goes as the magnehelic reading to the power b,

$$f(Q) = b * f(\Delta P)$$

For a typical reading $f(\Delta P) = .01/.35$. Thus the uncertainty in a single reading of the flow rate is

$$f(Q) = 0.44 * (.01/.35) = 0.013.$$

The conclusion is that the precision estimate of 2% is reasonable.

Table 3C.1: Flow audit summary (January 8-15, 1987)

Internal: flow rate calculated from IMPROVE magnehelic with readings by auditor
Audit: flow rate from orifice meter using water manometer (estimated uncertainty of 3%)
For each module: internal/audit = ratio

	Canyonlands	Hopi Point	Bullfrog	Page
A	20.2/20.0 = 1.01	20.7/19.1 = 1.09	21.0/21.2 = 0.99	21.6/20.4 = 1.06
B	20.7/20.4 = 1.02	10.7/12.8 = 0.83*	20.6/21.0 = 0.98	18.4/18.5 = 1.00
C	21.6/19.4 = 1.11*	20.7/21.0 = 0.99	21.1/21.4 = 0.98	20.9/20.4 = 1.03
D	22.2/22.7 = 0.98	21.5/20.4 = 1.06	21.7/21.8 = 0.99	19.9/18.9 = 1.06
E	20.6/20.4 = 1.01	21.9/21.4 = 1.02	22.4/21.4 = 1.05	19.5/19.7 = 0.99
F	20.4/19.1 = 1.06	20.0/18.7 = 1.07	21.1/21.2 = 1.00	20.2/19.7 = 1.02
special	20.8/21.0 = 0.99			19.1/18.7 = 1.02*

	Green River	Cisco	Monticello	Mexican Hat	Hite
K	21.1/21.2 = 0.99	20.2/20.6 = 0.98	21.4/20.6 = 1.04	21.3/21.6 = 0.98	21.3/21.4 = 0.99
L	21.4/21.8 = 0.98	21.1/20.2 = 1.05	22.7/22.7 = 1.00	20.7/20.8 = 1.00*	21.7/21.6 = 1.00
M	21.9/20.6 = 1.07	20.3/20.4 = 1.00	21.4/20.8 = 1.03	*	21.2/21.4 = 0.99
N	21.6/21.6 = 1.00	20.1/19.7 = 1.02	21.3/21.4 = 1.00	21.0/20.0 = 1.03	21.8/21.8 = 1.00

notes:

Canyonlands, module C: This was the only normal comparison exceeding 10%; the magnehelic readings by the auditor agree with those by UCD before and after sample collection.

Hopi Point, module B: The impregnated filter during this measurement had an extremely large pressure drop, the second largest at this site during the study. For a normal pressure drop, the ratio would probably be similar to other modules.

Page, special module: The values shown are based on readings done after the critical orifice had been changed. The audit flow rate for the original orifice was 16.8 l/min. The magnehelic reading for this first orifice by UCD personnel at 8 am (of 0.21 inches of water), gave a flow rate of 16.7 l/min, for a ratio of 0.99. On January 14 the orifice was replaced for the final time to give a normal flow rate near 21.7 l/min.

Mexican Hat, module L: The auditor was unable to get a valid reading on the magnehelic; the internal flow rate is based on logged readings by UCD personnel before and after the collection.

Mexican Hat, module M: The critical orifice was missing at the time of audit; it was installed on January 14. No valid audit was made for this module.

Precision and Accuracy of Analysis

Gravimetric Analysis

The primary measure of the precision of the gravimetric system is from the routine reweighing of control filters.[1] A blank filter is weighed in the morning and again in the afternoon. For the past three years, the standard deviation of the differences has been 4.5 μg.

One accuracy experiment was conducted weighing a series of paired blank filters on each of the three electromicrobalances of the UCD air quality laboratory. In all cases, the pairs were weighed at approximately the same time, so that there would be no problems with calibration changes. The resulting average standard deviation for the corresponding mass differences was 1.8 μg. Two conclusions were (1) that there was no significant difference between the results of the three balances and (2) that the major source of uncertainty must be changes in the calibration of the balance.

Precision tests have been run on the IMPROVE sampler at the Davis Field Station in which three or four identical Teflon filters were collected simultaneously. Figure 3C.1 shows the results for one such test with three samplers. The uncertainties were calculated assuming a flow rate uncertainty of 3% and an analytical uncertainty of 4 μg. The measured standard deviations were slightly smaller than the calculated precisions.

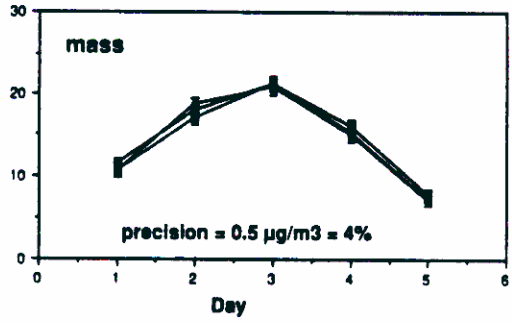

Figure 3C.1: Comparison of gravimetric mass by 3 side-by-side samplers at Davis.

PIXE Analysis

The precision of the PIXE analysis has both statistical and calibration components. The statistical precision depends on the number of counts in the x-ray peak and in the background under the peak. For concentrations near the minimum detectable limit, the statistical precision is around 45%. The calibration component is a constant fraction independent of the magnitude of the concentration. It is a combination of the uncertainties in the calibration standards and the beam charge. For large peaks the calibration component is much larger than the statistical component. The calibration standards are nominally rated at ±5%; by using a large number of standards and smoothing the results, the precision can be reduced to approximately ±2%. The normalization uncertainty can be estimated by precision tests using standard foils. For a series of analyses of single element standards the precisions were around 1%. The precisions for multi-elemental standards are slightly larger. These are shown in Table 3C.2. Note that these measurements were for peaks with enough counts so that statistical uncertainty was small. For repeated analysis of real samples over several months the uncertainty increases and precisions of around 4% are obtained.

Table 3C.2: PIXE calibration precision.

Based on analyses with sufficient statistics so that the major source of uncertainty is in normalization or calibration
Repeated analysis of single elemental standard (3/88)
Al 6 cases precision = 1.0%
Fe 6 cases precision = 1.2%
Pb 7 cases precision = 1.0%
Repeated analysis of multi-elemental standard (7 cases, 3/88)
Al precision = 5% (larger because of high SI)
Si precision = 2.7%
Ca precision = 2.3%
V precision = 4.2%
Mn precision = 3.3%
Repeated analysis of real samples over several months: For elements with negligible statistical uncertainty, such as sulfur, the average precision is 4%

For the WHITEX data we assumed the calibration precision to be 4%; the statistical precision was added to this quadratically. The total precision for the important elemental concentrations are given in Table 3C.3. This precision is a sum of the volume, calibration, and statistical components. The sum of the volume (3%) and calibration (4%) components is 5%.

Interlaboratory comparisons conducted periodically since 1975 have all shown that the UCD PIXE system provides results within the calculated uncertainty. Figure 3C.2 gives the results of an intercomparison conducted by RESOLVE between the UCD and NEA, who also analyzed the SCISAS samples.[2] The scatterplots show (1) excellent correlation, (2) intercepts that are very close to zero and (3) slopes that are close to but not precisely equal to unity. Similar results were obtained by the same two laboratories for the 1984 Reno intercomparison sponsored by SCENES.[3] The main difference here was that the slopes for Al and Si differed widely from unity. This emphasizes that the major source of error for x-ray systems (PIXE or XRF) is in the system calibration for each element. As long as the concentration is well above the analytical mdl, there is never a problem with intercept and there are few outliers. In the case of the Reno data, NEA found that their calibrations for Al and Si were incorrect.[4]

The samples of Figure 3C.1 were also analyzed by PIXE. The results are shown in Figure 3C.3. The precisions were calculated assuming a 3% precision in flow rate, a 4% precision in calibration, and the statistical precision determined by the analysis code. For most elements, such as S, Zn, Pb, Br and K, the measured precision is the same as the calculated precision. For Al, Si and Fe the precision is not as good as predicted. This is especially true for the last day, when the precision for all soil elements rises sharply. The problem is definitely not analytical, since the relative composition for all three samples on that day agreed precisely. Rather,the amount of soil

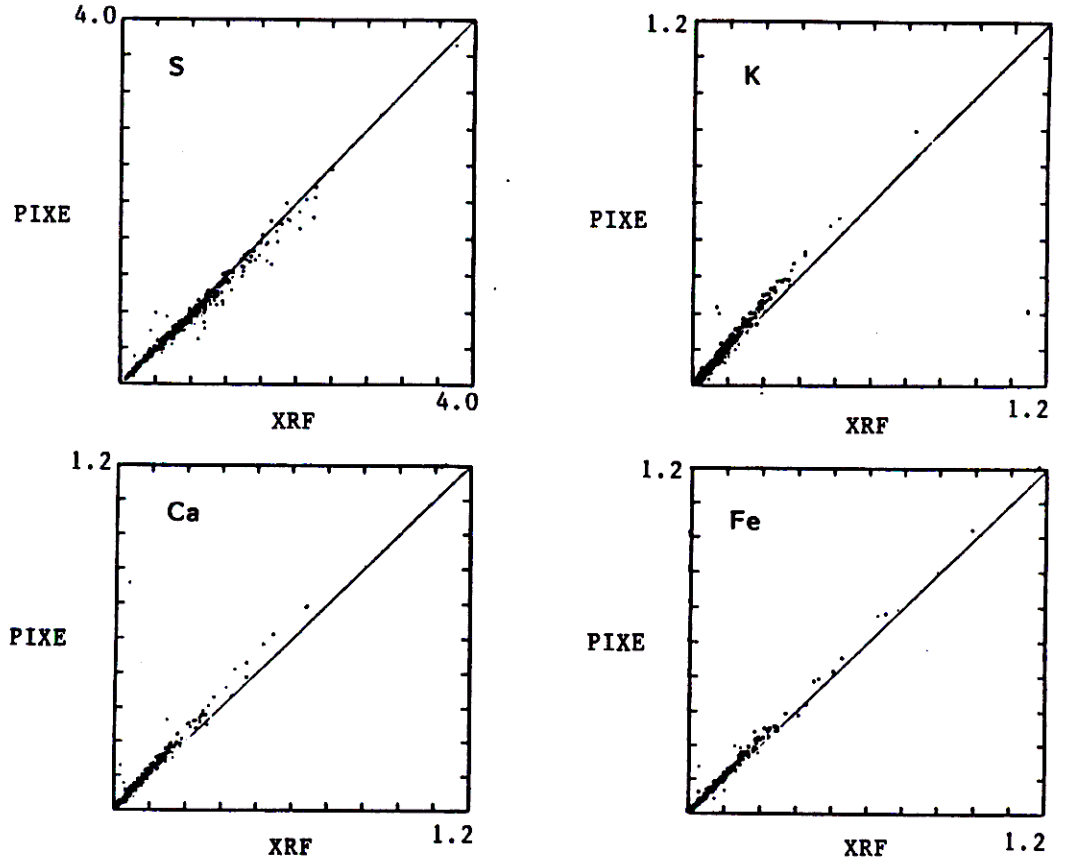

Figure 3C.2: Intercomparison between XRF (NEA) and PIXE (UCD) measured on parallel filters of 2 × 4 samplers in RESOLVE study.[2]

Table 3C.3: Average precisions for elemental concentrations with the IMPROVE sampler at Canyonlands, Hopi Point, Bullfrog, and Page. This precision is a sum of volume, calibration, and statistical components.

Variable	Time	Average Concentration ng/m^3	Average Uncertainty ng/m^3	% Precision
Al	6h	40.8	4.7	12%
Si	6h	44.2	3.3	8%
S	6h	262	13.9	5%
K	6h	29.3	2.6	9%
Ca	6h	12.5	1.5	12%
Fe	6h	13.0	1.0	8%
Fe	12h	11.3	0.6	6%
Ni	12h	0.45	0.10	23%
Cu	12h	0.46	0.09	19%
Zn	12h	1.26	0.13	11%
As	12h	0.68	0.14	20%
Se	12h	0.85	0.14	17%
Br	12h	1.08	0.18	17%
Pb	12h	2.13	0.41	19%

material on each sample was in fact different, although elements such as S and the total mass showed no such shift. We conclude that the measured precision is larger than the calculated precision for these soil elements because of collection uncertainty not included in the calculation. Two possible explanations are: (1) the ambient concentrations of some soil particles had large spacial gradients, or (2) the cutpoints of the cyclones were not identical and much of the soil mass was in particles near 2.5 μm. The Davis Field Station sat on a grass lawn, but was surrounded by open fields; much of the soil mass was generated locally and the large particles would not have had time to settle. The conclusion of the study was that the calculated precisions are generally correct, but can underestimate the actual precisions of soil particles when there is significant local soil contribution.

PESA Analysis

The precision of the PESA analysis is similar to that for PIXE in having statistical and calibration components. Based on reanalysis of actual samples, the PESA calibration precision is approximately 10%. For the average 12-hour F sample of 130 ng/m^3, the statistical precision was 6%, giving a total precision (volume, calibration,statistical) of 12%.

FAST Analysis

The precision of the PESA analysis is also a sum of statistical and calibration components. Based on reanalyses, the FAST calibration precision is approximately 10%. For the average 12-hour F sample, the statistical precisions for carbon, oxygen, and nitrogen were 20%, 8%, and 22%, giving total precisions (volume, calibration, statistical) of 22%, 13%, and 24%.

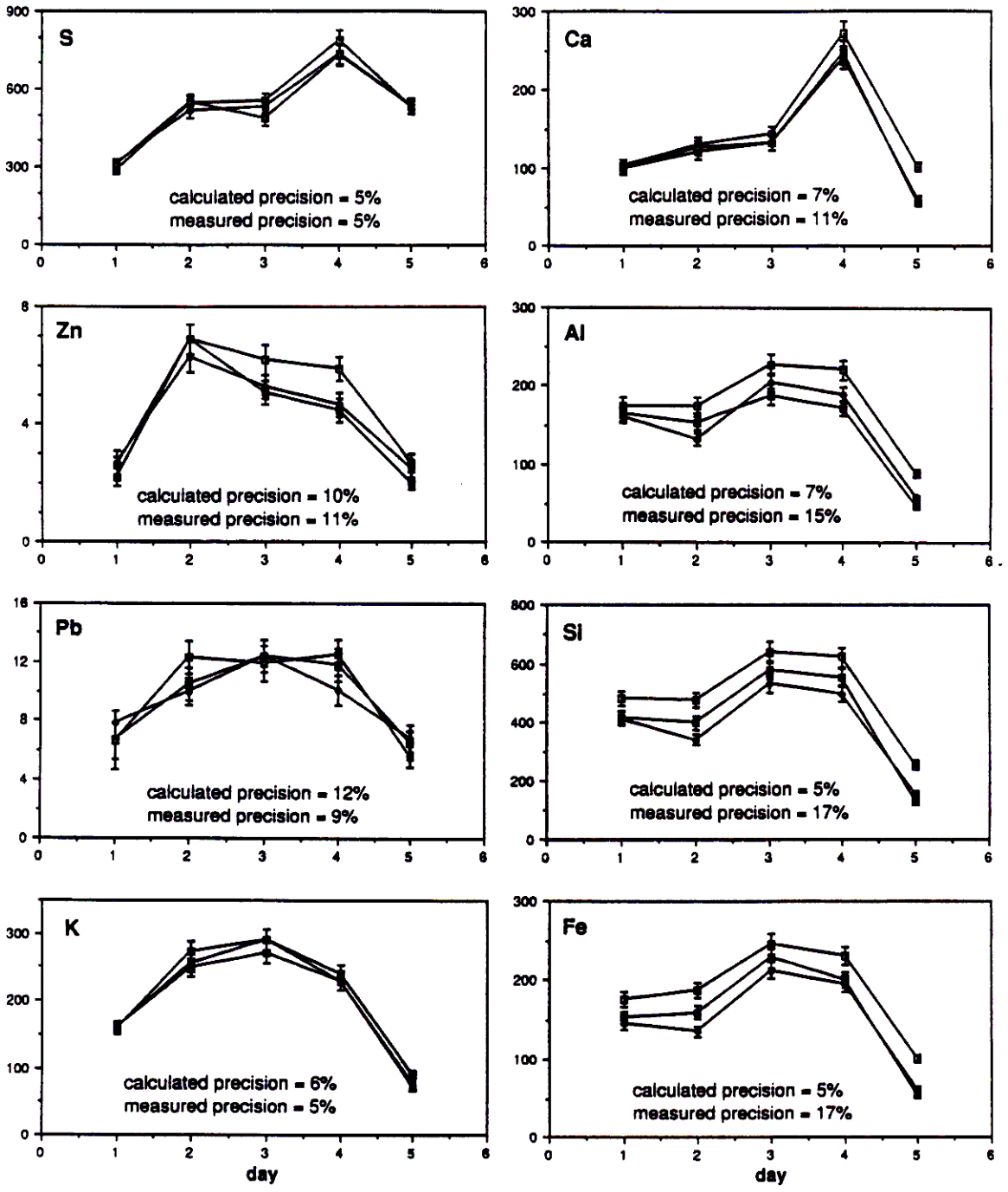

Figure 3C.3: PIXE precision at Davis Field Station. The calculated precisions include flow rate precision and are indicated by error bars. The measured precision is standard deviation/mean.

The carbon values are based on the average of three peaks in the spectra, elastic peaks from both detectors and an inelastic peak from the high-angle detector. Figure 3C.4 shows the standard deviation of the three measurements for a 10-day period.

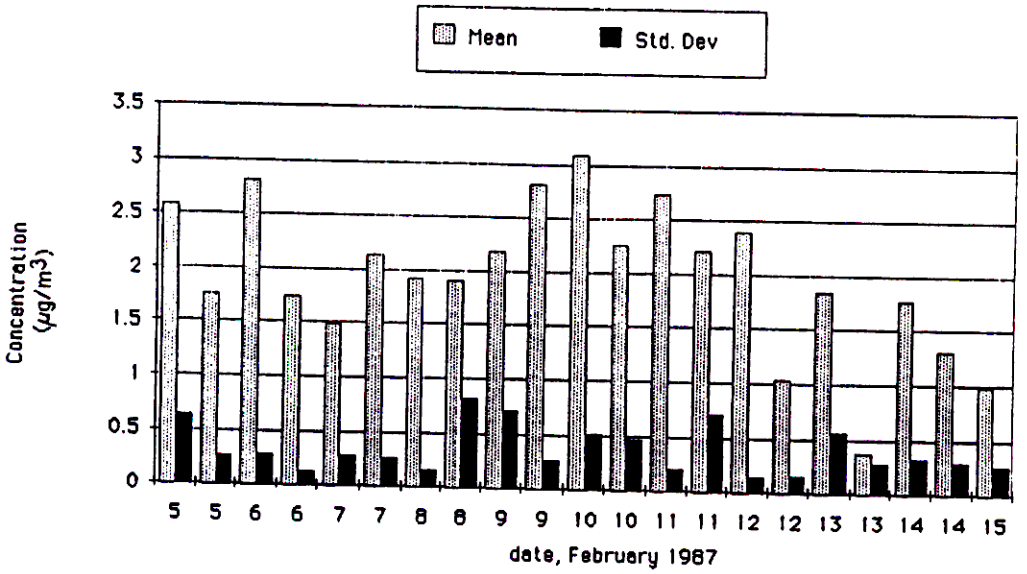

Figure 3C.4: Mean and standard deviation of three FAST measurements of total nonvolatile carbon; 62° elastic, 74° elastic, and 74° inelastic.

IC Analysis of Nitrate and Sulfate

The analytical protocols followed by Research Triangle Institute include (1) analysis of at least two standards each day with each IC analyzer, (2) routine analysis of the desorbing solution, (3) reanalysis of desorbed sample whenever the analysis is suspect, and (4) random reanalysis of desorbed samples.[5]

The two standards include aqueous solutions prepared by dilution of independently prepared stock solutions and EPA Acid Precipitation Audit samples with known values supplied by EPA. Comparisons performed after the WHITEX study using different dilution factors indicate that the uncertainty is proportional to the concentration. We have therefore assumed that the analytical precision is proportional to the measured value. This has significant implications for low and high concentrations; at low concentrations the minimum detectable limit will not depend on analytical uncertainty, but only on uncertainty of blank subtraction; at high concentrations the uncertainty is somewhat larger than would be the case if the analytical uncertainty were constant. The analytical precisions from the standards were found to be 3% for both sulfate and nitrate on Teflon, 4% for sulfate on nylon and 5% for nitrate on nylon.

Plots of 183 replicate analyses of IMPROVE network samples (in solution) are shown in Figure 3C.5. The rms average precision 3% for sulfate on nylon and 4% for nitrate on nylon. These are slightly better than the precisions estimated from the standards during the WHITEX analyses. These reanalyses also indicated that the uncertainty is proportional to the concentration rather than constant. For the WHITEX data base we used the estimates from the standards.

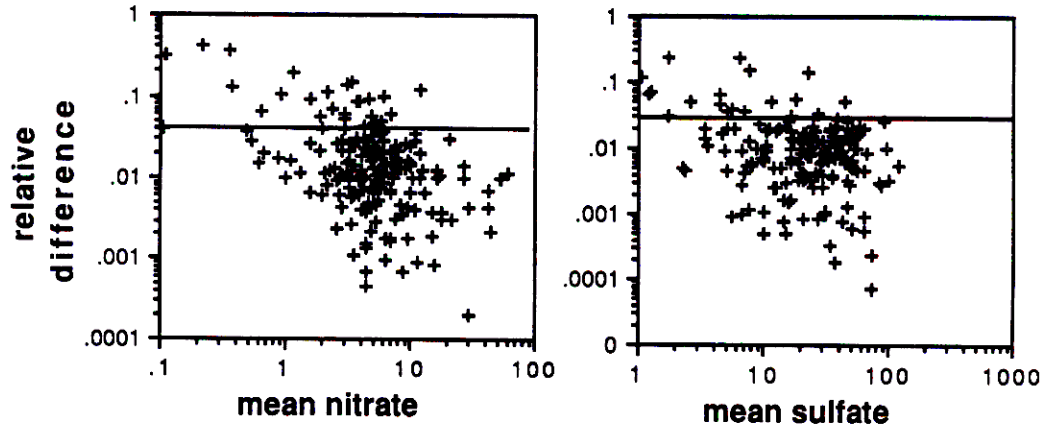

Figure 3C.5: Relative differences between replicate analyses for nitrate and sulfate data collected in IMPROVE network.

A side-by-side comparison was performed at the Davis Field Station with four modules; the results are shown in Figure 3C.6. Two modules (A,B) had only the bare aluminum tube used in all modules and the other two (C,D) had the concentric IMPROVE denuders. All samples were collected on nylon filters. Comparing the equivalent modules, the average precision was 4% for nitrate and 2% for sulfate.

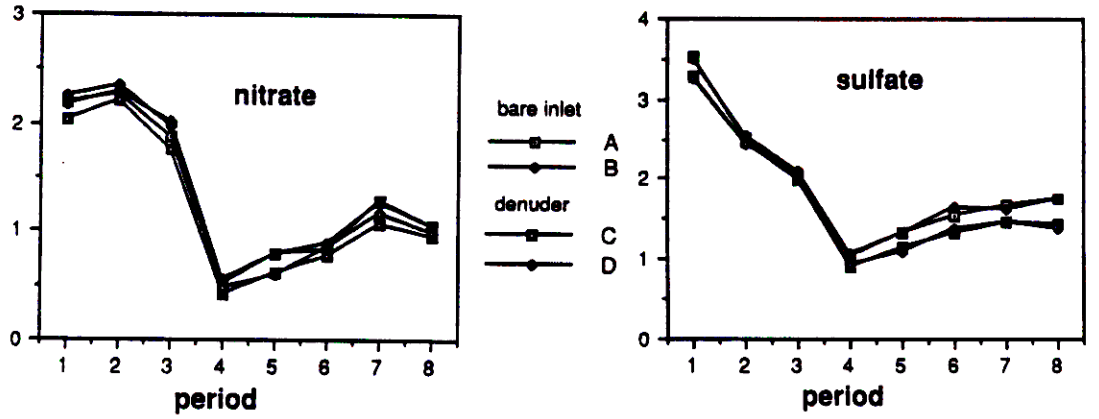

Figure 3C.6: IC precision at Davis Field Station; modules A and B have bare inlet without denuder and C and D have IMPROVE denuder.

TOR Analysis of Carbon

In the analytical protocol followed by DRI, punches are removed from the sample and analyzed.[6] Reanalyses are made by taking another punch from the sample. For the WHITEX, data replicate analyses were made on 45 samples. Figures 3C.7 and 3C.8 show that the analytical precisions for OC and LAC are independent of the measured values. The precision for paired measurements is defined as the difference divided by $\sqrt{2}$. The RMS average precision for the two variables are 1.87

and 1.21 μg. Because the precision in the analysis is not zero for clean filters, the precision must be included in the calculation of the mdl.

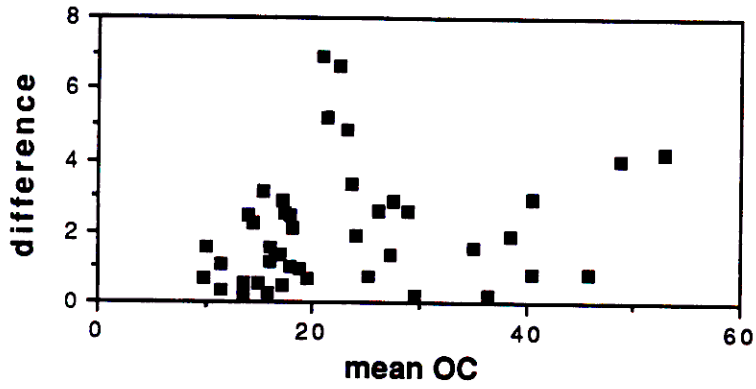

Figure 3C.7: Differences between organic carbon reanalyses.

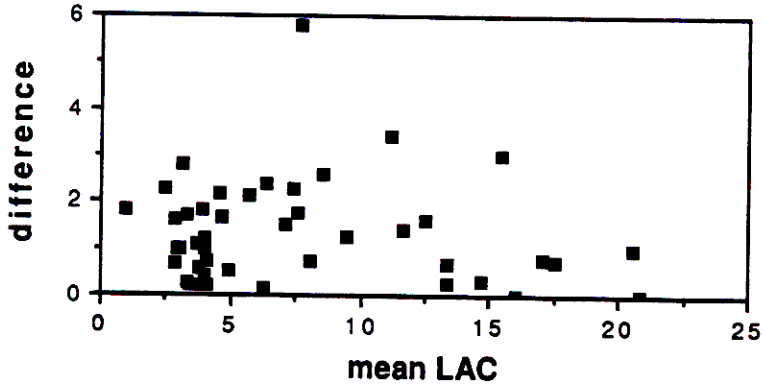

Figure 3C.8: Differences between light-absorbing carbon reanalyses.

The accuracy of the analyses can be estimated from the intercomparison conducted in 1986 by the California Air Resources Board.[7] The conclusion appears to be that the measurements sometimes differ considerably between analytical methods, such as TOR and TMO, especially for "elemental carbon", often depending on the source of the organic material.

Value, Precision, and Accuracy of Artifacts

A positive artifact is defined as any contamination that is falsely measured as ambient material. A negative artifact denotes sampling loses during collection and handling. We did not conduct any tests to evaluate negative artifact during WHITEX; therefore we will use the term artifact to mean only positive artifact. There are several possible sources of artifact.

- The analysis may introduce a contaminant.
- The filter material may contain the measured species.

- The filter may acquire an artifact from contact with O-rings and other components of the collection system, or from travel.
- The filter may adsorb undesired gases during collection. Note that adsorption of gases is not an artifact if the gas is included as part or all of the measured values.

Measurements of different types of blanks are needed to identify the sources of artifact: solution blanks (for IC), laboratory blanks, travel blanks, dynamic field blanks, and backup filters. In general, one uses the differences between the types of blanks to identify a given source. Our approach in this section is to include as much data as possible to specify the total artifact, but exclude all blanks from the final calculation that do not incorporate all sources of artifact. For example, dynamic field blanks can be combined with backup filters if the data indicates that there is no gas adsorption.

Gravimetric Mass

The mass artifact for the SFU and IMPROVE networks is monitored using a control filter protocol that involves weighing a clean filter each day, loading it into a cassette, keeping it on the shelf for one month, and reweighing it. During the period covering the WHITEX gravimetric analyses (12/86 to 4/87), the average control gain was 4±5 μg. Tests indicate that this gain appears soon after loading. Dynamic field blanks (filters loaded into the IMPROVE sample but not run) for the IMPROVE network for the first half of 1988 show that the sample does not add any further artifact.

The average field blank for the WHITEX IMPROVE sites had a mass gain that was much larger than the control gain. The 11 dynamic field blanks gained 12 μg, which was 3 times the control value. The problem was especially great at Page, where the 5 field blanks gave an average gain of 15±9 μg, with values of 3, 8, 19, 21, and 24 μg. At the other WHITEX-IMPROVE sites the field blanks averaged 9±4 μg. The only possible explanations for the large gain was that the cassettes were loaded and unloaded in apartment rooms rather than at the UCD laboratory. No mass gain was observed for filters that remained in Petri dishes at the WHITEX sites for the duration of the study.

The large artifact was also observed in the regressions of mass against reconstructed mass and hydrogen. The intercept at Page indicated an artifact of 21±10 μg. A small artifact of 6 μg was indicated for Hopi Point. The artifacts and their uncertainties used for the WHITEX data are summarized in Table 3C.4.

Table 3C.4: Mass artifact for IMPROVE samples.

Hopi Point	6 ± 6 μg
Page	15 ± 9 μg
All others	9 ± 6 μg

The large uncertainty in the mass artifact, in combination with low ambient concentrations and short durations, resulted in large relative precision for the mass concentration. For the 12-hour F filters, the uncertainty from the mass artifact is 15% of the average mass concentration. For the 6-hour filters, this is 30%. Because of this large uncertainty for the 6-hour concentrations, we have chosen to invalidate the 6-hour mass data and use only the 12-hour mass concentrations.

PIXE and PESA

Analysis of field blanks by both PIXE and PESA show no elemental artifacts on the Teflon filters.

IC Analysis of Nitrate and Sulfate

The artifact values to be subtracted from the IC results were determined from three types of blanks:

1. desorbing solution—analysis of the solution used in IC analysis
2. field blanks—filters that had been placed into cassettes and loaded into the cyclone manifold, but no air had been drawn through
3. second filters—backup filters in nylon-nylon pair.

The assumptions were that the artifact values did not change with site or time. We also assumed that the denuder and nondenuder nylon had the same artifact. The values are given in Table 3C.5. The "chosen artifact" is the value chosen for the WHITEX data. For nitrate on nylon, this is an average of the field blanks and the secondary filters, since the two are statistically equivalent. The similarity between the secondary filters and the field blanks also indicates that the first filter removed 100% of the nitric acid vapors. For nitrate on Teflon, only the field blanks were used since there is an artifact associated with the filter and/or cassette. The uncertainty of the desorbing solution was used, since the spread of the field blanks appears to be too small. For sulfate on Teflon, the chosen average is an average of both desorbing solution and field blanks since they are statistically equivalent. For sulfate on nylon, there appears to be an adsorption artifact contribution, so only the 2nd filter is used. There was no correlation between the sulfate on the 2nd filter and either the sulfate on the 1st filter or the SO_2 concentration.

Table 3C.5: Nitrate and sulfate artifacts, in $ng/filter$.

	Nitrate		Sulfate	
	nylon	Teflon	nylon	Teflon
Desorbing solution	880 ± 214	281 ± 148	1362 ± 1141	105 ± 79
Field blanks	1300 ± 738	858 ± 27	1413 ± 653	188 ± 43
2nd filters	1322 ± 496	—	2088 ± 587	—
"Chosen artifact"	1316 ± 576	858 ± 145	2088 ± 607	122 ± 79

TOR Analysis of Carbon

There are three sources of artifactual carbon mass: (1) contamination in the blank quartz filters, (2) contamination of the filters in the petri dishes or in the cassettes, and (3) artifact due to adsorption of organic gases, primarily during sampling.

Four laboratory blanks that had not been put into cassettes and four field blanks that had been installed in the sampler were analyzed. The problem with the field blanks is that 1 of the 4 gave

extremely high organic carbon mass compared to the others and to many actual samples. This filter was reanalyzed and the same approximate value was obtained. No explanation for this was determined. This value was dropped from the calculation of the average field blank, but is raises the possibility that some of the samples may have more artifact than estimated. To estimate the artifact caused by adsorption of organic gases, an extra module was used at Page which collected 24-hour double quartz samples. The measurements on the second filter should be the sum of a field blank plus the gas artifact. The values for the three categories of artifacts are given in Table 3C.6.

Table 3C.6: Carbon artifacts, in $ng/filter$.

	Organic	Light Absorbing
Laboratory blanks	6350 ± 1630	210 ± 210
Field blanks	8650 ± 1830	1910 ± 400
2nd filters	14510 ± 3070	2140 ± 1670
"Chosen artifact"	14510 ± 3070	2120 ± 1590

The contributions from different sources of artifact can be estimated by examining the differences between the averages in the table. For organic carbon, the quartz filter (and possibly the Petri dish and analysis) contributes 6 μg, the cassette contributes 2 μg, and gas adsorption contributes 6μg. Because of the large gas artifact, the chosen artifact is based solely on the average of the second filters. The use of single value for the chosen artifact assumes that the gas adsorption saturates all filters equally. This requires that the adsorption process depends only on the filter material and will not exceed the saturation value even if the ambient organic gas concentrations are high. It also requires that the ambient organic gas concentrations are high enough to produce saturation. These will be discussed below. For light-absorbing carbon, nearly all of the artifact is contributed by the cassette. Because there is no gas artifact for LAC, the chosen artifact is based on the average of both field blanks and second filters.

There are two difficulties with the gas artifact value obtained at Page. First, the double quartz filters were run for 24 hours, while the normal quartz filters were run for 12 hours. It was necessary to determine whether the 24-hour artifact was equal to or double the 12-hour artifact. This was determined by comparing the masses on the two 12-hour samples with the first stage of the corresponding 24-hour sample. If the sum of the two 12-hour masses minus the 24-hour mass equals the normal value of a field blank, then the 24-hour artifact is twice the 12-hour one. If, however, the difference equals the normal value of the second filter, then the artifact saturated during the first 12 hours and no additional artifact was formed during the second 12 hours. To compensate for slight variations in volume, due to variations in both flow rate and sample duration, the masses were normalized to the volume of that filter. The results clearly show that saturation occurred in 12 hours.

field blanks	8.7 ± 1.8 μg
2nd filters	14.5 ± 3.1 μg
parameter	14.6 ± 3.6 μg

The second difficulty with the special sampling at Page is that this site is close to a town and possible sources of organic gases and the results may not be applicable to sites where the ambient organic gases might be less. At Hopi Point the measured OC was less than the chosen artifact on 40% of the samples, while at Canyonlands and Bullfrog it was less on 16% of the samples and at Page on 2%. A possible explanation was that the gas artifact did not always saturate during the 12-hour sample at Hopi Point. The correct artifact would then lie somewhere between 9.0 and 14.5 μg.

The large uncertainty in the chosen artifact plays a significant role in evaluating the usefulness of the carbon data. For the 12-hour samples, the OC uncertainty of 2.1 μg corresponds to 0.20 $\mu g/m^3$, while the LAC 1.6 μg corresponds to 0.11 $\mu g/m^3$. For all primary sites, these uncertainties were 40% of the average OC and LAC concentrations. The situation was especially acute at Hopi Point, where almost every OC and LAC concentration was less than 2σ. This can be seen in the time plots comparing the alternate methods of determining organic mass (Figure 3C.9) and light-absorbing carbon (Figure 3C.10. The dashed lines give the 2σ values for the variables determined by TOR. For the WHITEX data it is necessary to use the organic estimates from hydrogen and the LAC estimates from the coefficient of optical absorption.

FAST Analysis of C, O, and N

The FAST mdls are defined in the same way as for PIXE and PESA. The average mdls for carbon, oxygen, and nitrogen were 620, 100, and 120 ng/m^3, respectively. The concentrations were above mdl for 75% of the measurements of carbon and nitrogen, and 95% of oxygen.

Values of Precision Factors

The precision of variables measured by IC, TOR, and gravimetric analysis are the quadratic sum of precision factors associated with flow rate, artifact subtraction, and analysis. The artifact precision is always independent of the concentration and the flow rate precision is proportional to the concentration. The analytical precision was found to be proportional for IC and constant for the other.

The total precision of the concentrations for the WHITEX was calculated from the following equation:

$$\sigma(\text{conc}) = \sqrt{(\sigma_b/V)^2 + (\sigma_m/V)^2 + (f_V c)^2 + (f_m A/V)^2},$$

where σ_b and σ_m are the constant precisions in artifact and analysis and f_V and f_m are the relative precisions in flow rate and analysis. The values used for these factors in the WHITEX data are given in Table 3C.7.

Minimum Detectable Limits

Gravimetric Analysis of Mass

The minimum detectable limit for gravimetric is defined as twice the uncertainty in the chosen artifact. For sites other than Page, the mdl of 12 μg/volume is equivalent to a concentration of 1.6 $\mu g/m^3$ for the 6-hour A filters and 0.8 $\mu g/m^3$ for the 12-hour F and X filters. For Page, the mdl's are 50% higher. Because of this large mdl for the A filters, only 57% of the filters had masses above the mdl. For this reason, the mass concentrations on the A filters were invalidated. The F filters had 88% of the masses above the mdl, and the X filters (secondary sites) had 92%.

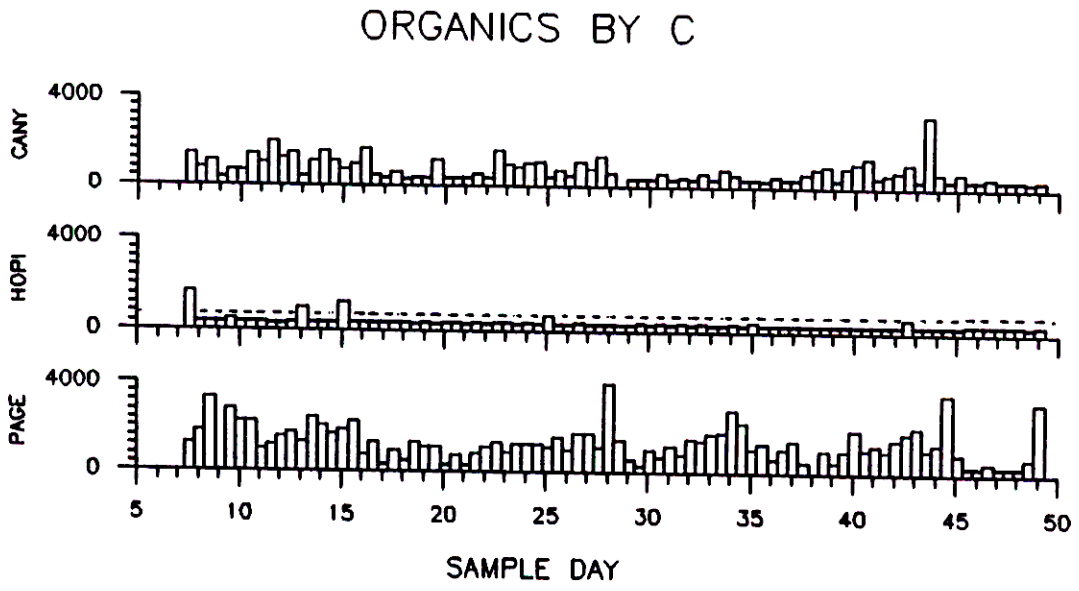

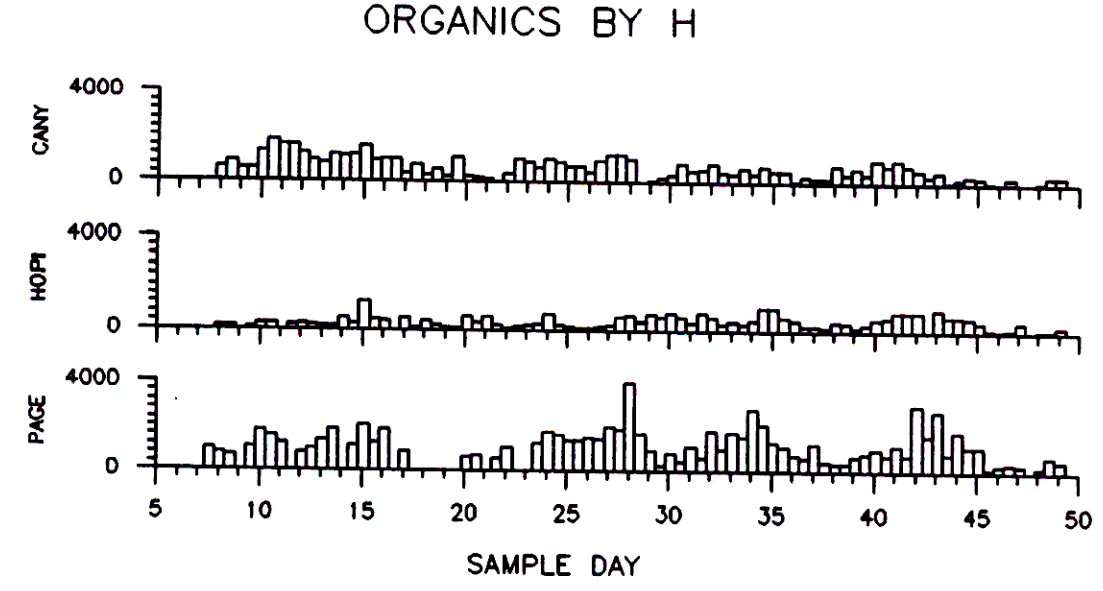

Figure 3C.9: Time plots of organic mass for Canyonlands, Hopi Point, and Page. The upper set was calculated from OC by TOR and the lower set from H by PESA. The dotted lines for the upper Hopi Point indicate the minimum detectable limits.

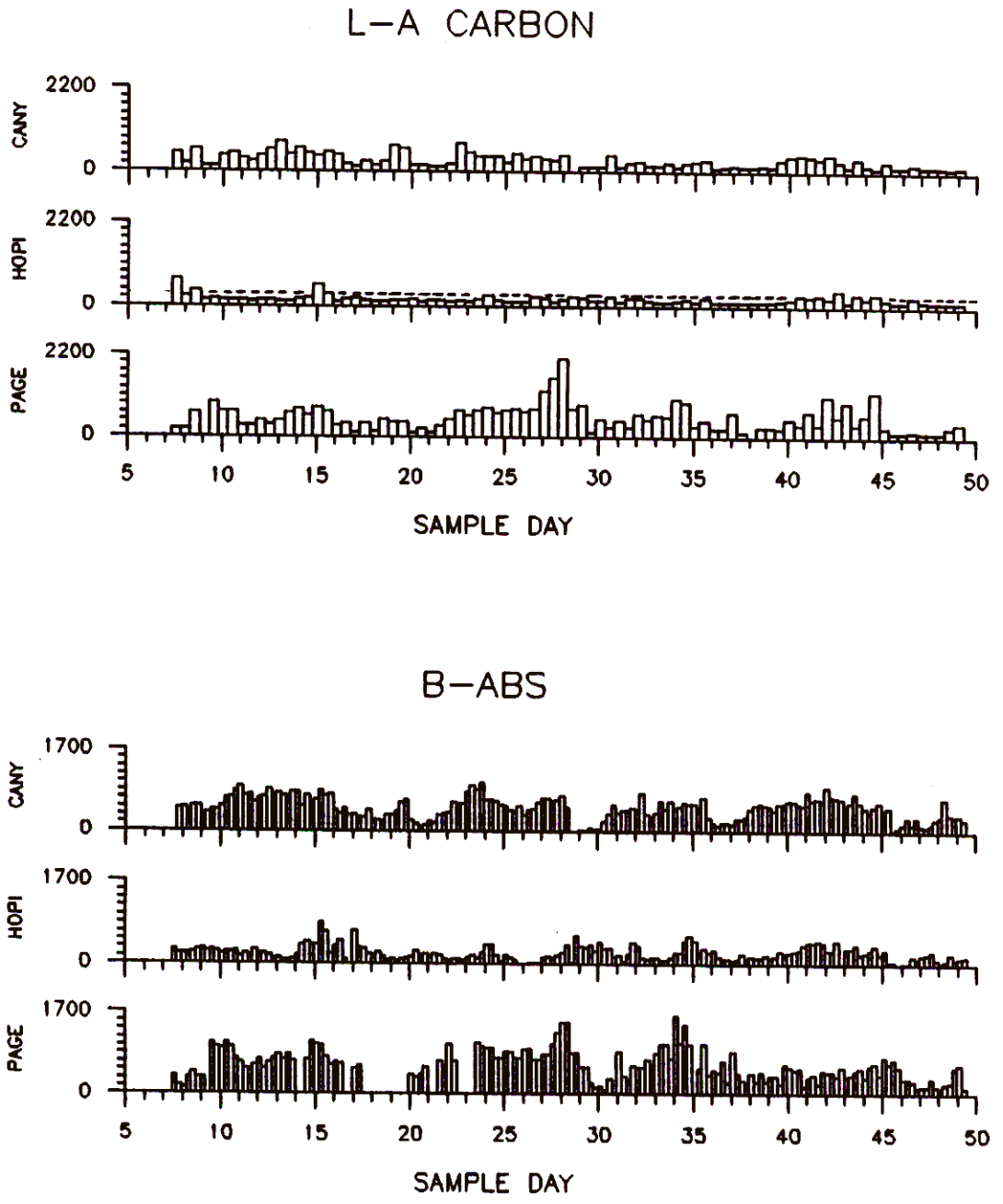

Figure 3C.10: Time plots of light-absorbing carbon for Canyonlands, Hopi Point, and Page. The upper set was calculated from EC by TOR and the lower set from absorption by LIPM (assuming efficiency of 10 m^2/g). The dotted lines for the upper Hopi Point indicate the minimum detectable limits.

Table 3C.7: Factors used to calculate precision of concentrations.

	Constant (μg)		Relative	
	artifact	analysis	flow	analysis
	σ_b	σ_m	f_V	f_m
B–SO_4	0.079	.0	.03	.03
D–SO_4	2.088	.0	.03	.04
E–SO_4	2.088	.0	.03	.04
B–NO_3	0.145	.0	.03	.03
D–NO_3	1.316	.0	.03	.05
E–NO_3	1.316	.0	.03	.05
S–SO_2	0.676	.0	.03	.07
C–OC	3.07	1.87	.03	.00
C–LAC	2.12	1.59	.03	.00
F–mass, X–mass[1]				
Page	9.0	.0[1]	.03	.00
Others	6.0	.0[1]	.03	.00

F–mass, X–mass[1]: σ_m included in σ_b.

PIXE Analysis of Elements

The minimum detectable limits for PIXE are derived for each element from the x-ray spectrum. It is the concentration that would result if the number of counts for the defining peak were equal to 3.29 times the square root of the number of counts in the background under the peak. The average minimum detectable limits for the various IMPROVE filters and percentage of time that the element was detected above mdl are given in Table 3C.8.

Table 3C.8: Average minimum detectable limits for PIXE in ng/m^3 and percent of times element found.

	6-hour A	12-hour F	12-hour X
Al	2.9 (80%)		
Si	2.0 (100%)		1.9 (97%)
S	2.0 (100%)		1.4 (100%)
K	1.7 (100%)		1.2 (87%)
Ca	1.4 (94%)		1.1 (100%)
Ti			1.0 (33%)
Mn			0.63 (13%)
Fe	1.0 (96%)	0.24 (100%)	0.40 (99%)
Ni		0.23 (60%)	0.42 (49%)
Cu		0.17 (64%)	0.28 (43%)
Zn		0.16 (94%)	0.24 (93%)
As		0.16 (36%)	0.27 (50%)
Se		0.18 (31%)	0.30 (34%)
Br		0.20 (73%)	0.36 (62%)
Rb		0.29 (2%)	0.51 (3%)
Sr		0.37 (17%)	0.68 (7%)
Zr		0.47 (22%)	0.80 (12%)
Pb		0.46 (45%)	0.82 (29%)

PESA Analysis of Hydrogen

The PESA mdl is defined in the same way as those for PIXE. The average mdls for hydrogen were 29 ng/m^3 for the A filters, 10 ng/m^3 for the F filters, and 15 ng/m^3 for the X filters. Hydrogen was detected in 91% of valid samples at all sites. The PESA system has been revised since the WHITEX analyses, resulting in considerably lower limits.

IC Analysis of Nitrate and Sulfate

The minimum detectable limits for nitrate and sulfate are defined as twice the uncertainty for a sample that is blank. For IC the mdl is twice the uncertainty in the blank subtraction. For the average Teflon filter this is 40 ng/m^3 for nitrates and 22 ng/m^3 for sulfates. Sulfate was measured above the mdl on nearly all samples, while nitrate was above mdl on only 32% of the samples, because of the low collection by Teflon. The mdl's were 80 ng/m^3 for both nitrate and

sulfate on the 12-hour D filters and 40 ng/m^3 on the 24-hour E filters. For both filters the nitrate concentration was above mdl on 85% of the samples, while sulfate was almost always above.

TOR Analysis of Carbon

The minimum detectable limits for the two carbon species are also defined as twice the uncertainty for a sample that is blank. Because the analytical uncertainty does not depend on the amount of material in the sample, the mdl is twice the quadratic sum of the uncertainties in the blank subtraction and in the analysis. For the average filter this is 490 ng/m^3 for organic carbon and 270 ng/m^3 for light-absorbing carbon. Because of these large mdl's, OC is found above mdl on only 40% of the filters and LAC on only 48%. At Hopi Point neither parameter was found often enough to be useful.

Internal Comparisons

Particulate Mass and Hydrogen

Hydrogen is present as a 6–10% component of ammonium sulfate and organics and is absent in soils and elemental carbon. As long as soils and elemental carbon are a small portion of the fine aerosol, there will be good correlation between mass and hydrogen. In the NPS network with SFU's the correlation for all sites was 0.82 and hydrogen accounted for 4% of the mass. The comparison for all nine IMPROVE sites in WHITEX is shown in Figure 3C.11. (See Appendix 3G for discussion of perpendicular regression and data accompanying the plots.) The hydrogen is multiplied by 25 for convenience. The correlation was 0.90 and hydrogen accounted for 5% of the mass.

Sulfur/Sulfate

The first two modules (A and B) at Canyonlands, Hopi Point, Bullfrog, and Page collected 6-hour samples on Teflon. A was analyzed for S by PIXE and B for $SO_4^=$ by IC. For comparison, the S values were multiplied by 3.0 to give equivalent SO_4 concentrations. Figure 3C.12 compares the fit of Page and Figure 3C.13 the fit for all data. The correlation for all data is 0.94 and the slope is 1.07 $\pm$ 0.03. The average difference of 113 ng/m^3 at Page was slightly larger than the difference predicted from the propagated precisions of 71 ng/m^3.

The sulfate on the two nylon filters, D without a nitrate denuder and E which correlate well with each other and with both Teflon filters. The fit between the D filter and a parallel "Z" quality assurance filter at Canyonlands is shown in Figure 3C.14. The average difference of 54 ng/m^3 was less than the pedicted difference of 84 ng/m^3. Figures 3C.15 and 3C.16, show that the nylon sulfate values are slightly higher than the Teflon values, probably because of adsorption of sulfur gases on the nylon filter. The indication from our current monitoring is that the differences increase with the temperature and SO_2 levels. Nevertheless, the nylon filter provides a good quality assurance check for the Teflon sulfate.

Soil Elements

Iron was the only soil element that was measured on both the 6-hour A and the 12-hour F Teflon filters. The fit for all data is shown in Figure 3C.17. The correlation of 0.92 is good, considering the short duration of the samples and the low ambient concentrations. The slope is within 1 standard deviation of unity. The average difference at Page was 1.4 times the difference predicted from the propagated precisions.

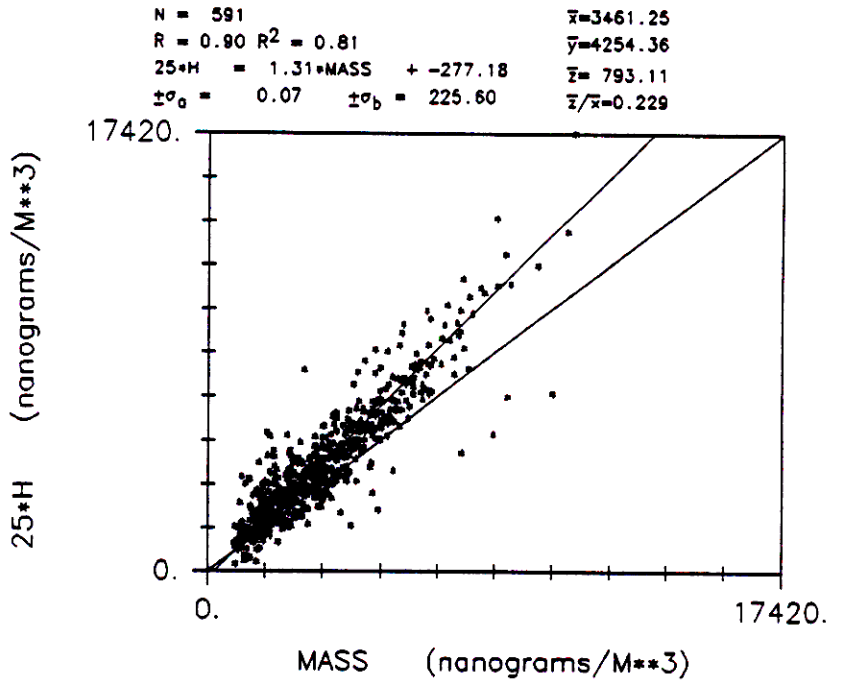

Figure 3C.11: Comparison of hydrogen and gravimetric mass at all nine sites. The multiplicative factor for H is for convenience.

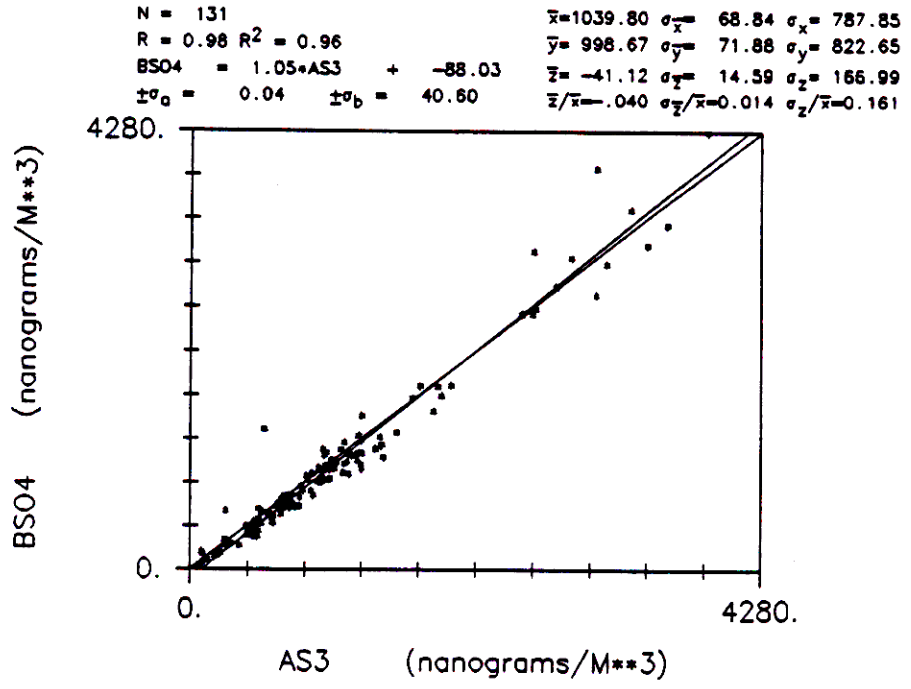

Figure 3C.12: Comparison of sulfate on Teflon by IC and sulfur times 3 on Teflon by PIXE at Page.

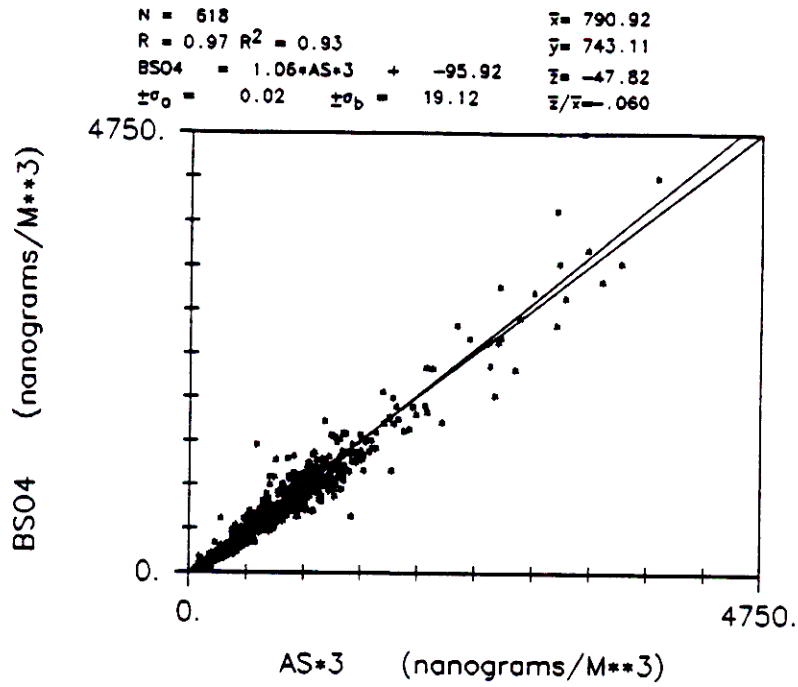

Figure 3C.13: Comparison of sulfate on Teflon by IC and sulfur times 3 on Teflon by PIXE at Canyonlands, Hopi Point, Bullfrog, and Page.

Nitrate

A special quality assurance module with nylon filters and no denuder was operated at Canyonlands. The fit between this filter and the standard D filter with no denuder is shown in Figure 3C.18, where "Z" is the QA filter. The average difference of 54 ng/m^3 was less than the predicted difference of 84 ng/m^3.

Carbon

A special quality assurance module was operated at Page with double quartz filter cassettes. The fits between the normal filters (C) and the first of the QA filters (H) are shown in Figure 3C.19, and 3C.20, along with error bars showing the average uncertainties. The correlations of approximately 80% are reasonably good considering the large uncertainties in the 12-hour variables. The average differences of both variables were 30% smaller than the differences predicted from the propagated precisions. The comparison between LAC and the coefficient of optical absorption is discussed in Appendix 3F.

The organic concentrations estimated from hydrogen from filter F and sulfur from filter A provide a comparison for organic carbon from filter C by the TOR method. The calculation is discussed in Appendix 3A.1. The equations for organic mass are

$$OMH = 11 * (H - 0.25 * S)$$

$$OMC = 1.4 * OC.$$

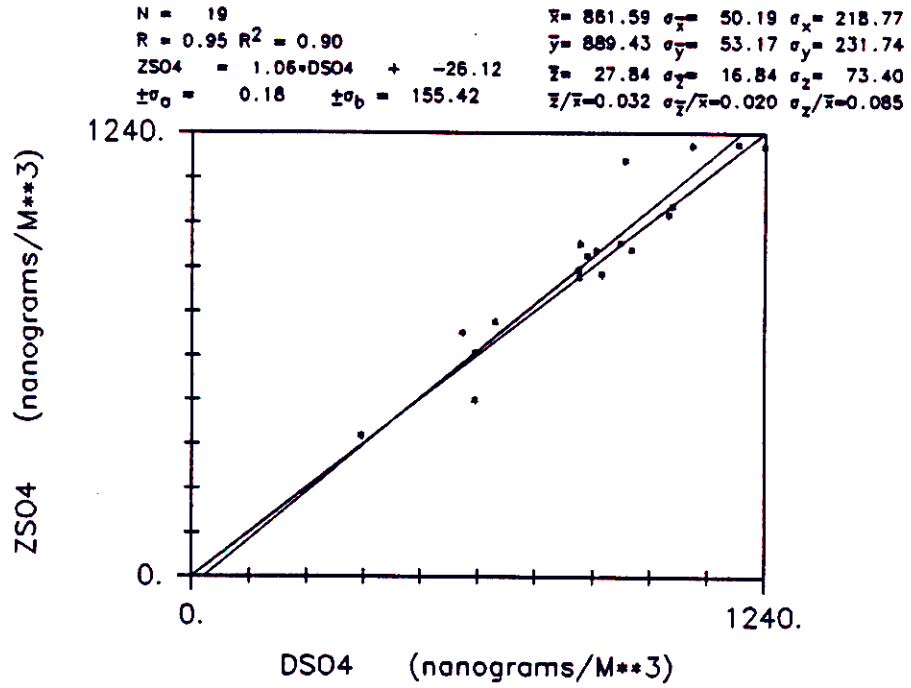

Figure 3C.14: Comparison of sulfate on special module and sulfate on normal module at Canyonlands. Both modules have nylon filters without denuders.

The upper plot Figure 3C.21 shows the comparison for Page. The correlation is poor (r =0.4), although the average concentrations are similar. The problem is the relatively large uncertainty in the TOR measurements for 12-hour samples. Comparisons for the other sites cannot be made because of the relative uncertainty is even larger. The comparison has been repeated for the IMPROVE network. The lower portion of Figure 3C.21 shows the comparison for all western sites for samples collected during fall 1988.[8]

Reconstructed Mass

One test of the collection and analysis is the agreement between measured and reconstructed mass. The reconstructed mass includes sulfate, soil, nonsoil potassium, elemental carbon, organic matter and nitrate. It does not include volatile species or water The soil equation is

$$\text{soil} = (Al * 1.89 + Si * 2.14 + CA * 1.40 + Ti * 1.67 + Fe * 2.2)/0.86$$

where soil potassium is included in the iron factor and the 0.86 factor compensates for other components that contribute an additional 14% of the total mass of sediment. An equivalent equation for soil of iron times 20 was used in the model analyses. (The factor of 20 is consistent with crustal averages and with historic records for fine soils on the SFU sampler. The comparison for WHITEX is shown in Figure 3C.22.) Potassium must be excluded from the equation for soil because much of it came from nonsoil sources, especially at Canyonlands and Bullfrog. Figure 3C.23 shows that the potassium concentration is generally well above the soil relationship that $K/Fe = 0.70$. However, the nonsoil potassium was included in the reconstructed mass as a separate component. The nitrate term ($NO_2 * 1.29$) should be based on the nitrate measured on Teflon, if the primary concern is

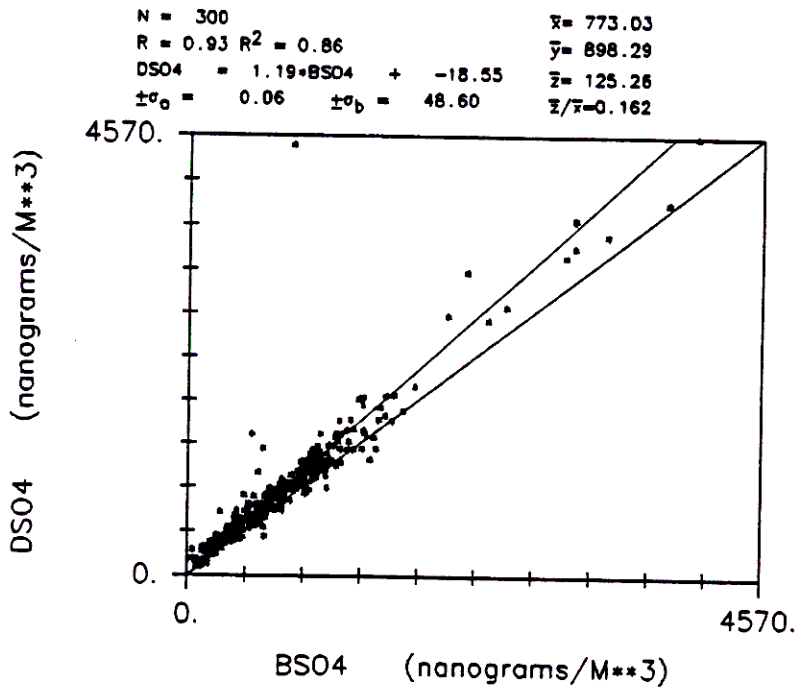

Figure 3C.15: Comparison of sulfate on nylon (without denuder) and sulfate on Teflon at Canyonlands, Hopi Point, Bullfrog, and Page.

comparing reconstructed mass to the mass that remains in the Teflon filter. For Page, using the particulate nitrate concentration (module E) would incorrectly add 5% to the mass, while using the total nitrate (module D) would add 10%. The SCISAS total nitrate is even higher and would add 18%. The sulfate term assumes fully neutralized $(NH_4)_2SO_4$, from PIXE S times 4.125. The two carbon components are estimated from hydrogen (OHM) and absorption, because the quartz method does not give enough sensitivity. At Page a second estimated reconstructed mass is based on the quartz values.

The comparison for mass *vs* reconstructed mass using the quartz carbon (RMC) is shown in Figure 3C.24, while that using H and absorption (RNH) is shown in Figure 3C.25. The fit is somewhat better with RNH ($r = 0.96$ *vs* $r = 0.86$). The fit does not precisely pass through the origin, suggesting that we could have increased the mass artifact to 21 μg. The slope is nearly, but not quite, unity; a 2% contribution for water would increase it to 1.00. A similar plot for all primary sites in Figure 3C.26 shows that the intercept is zero overall and that the reconstructed mass accounts for 90% ± 5% of the mass.

FAST Data

The measurements of carbon, oxygen, and nitrogen, along with the PIXE and PESA measurements, provide an additional check of the mass balance of the samples. The first comparison, shown in Figure 3C.27, compares the nitrogen and sulfur concentrations. If all the nitrogen were present as ammonium sulfate, the slope would be 0.88. The best fit gives a small intercept and a slope close to 0.88. The comparison indicates that ammonium is the dominant source of nitrogen on the filter.

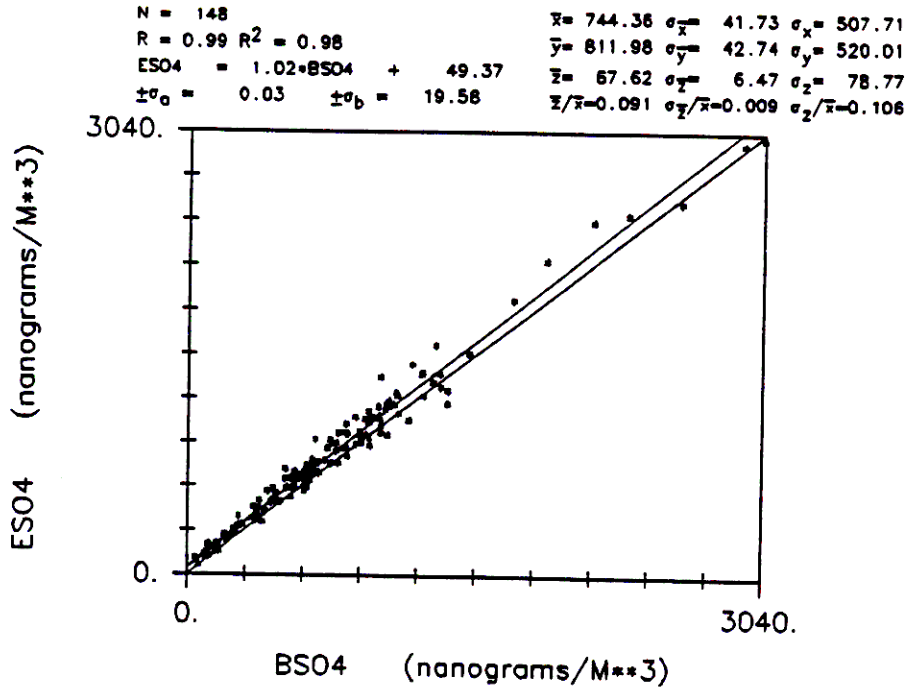

Figure 3C.16: Comparison of sulfate on nylon (with denuder) and sulfate on Teflon at Canyonlands, Hopi Point, Bullfrog, and Page.

It indicates that most of the nitrogen associated with the ammonium nitrate had been volatilized from the filter before the FAST analysis.

The second comparison is between the measured oxygen and the oxygen predicted from the sum of soil, sulfate, and organic components. Figure 3C.28 shows that the average slope is close to the predicted 1.

The final comparison is between the mass and the sum of all elements from FAST, PIXE, and PESA, shown in Figure 3C.29. The relatively small correlation coefficient is a result of the relatively large imprecision in the carbon concentrations of approximately 22%. However, the average ratio is close to 1, indicating that all of the mass is accounted for.

3C.3 DRUM Sampler

Estimated Precision and Accuracy of Air Volume

The flow rate for the DRUM sample is set by the final orifice (stage 8), which operates at criticality, and varies only with the square root of the absolute temperature. This gives a flow rate of 1.1 l/m at STP. This flow is verified operationally by two gauges. The first is a 0 to 1" H_2O minihelic between stages 1 and 2, which is used to measure the flow rate. The second is a vacuum gauge behind stage 8, which verifies that the stage 8 orifice is operating at criticality. The minihelic was calibrated using an orifice gauge placed over the intake; the orifice meter was calibrated by a Collins Integrating Spirometer at Davis and corrected for altitude and temperature.

The flow rate of each DRUM sampler in WHITEX was audited four times, three by UCD and once by ERT. The flows were found for all units at WHITEX to be ±3.5% of nominal values.

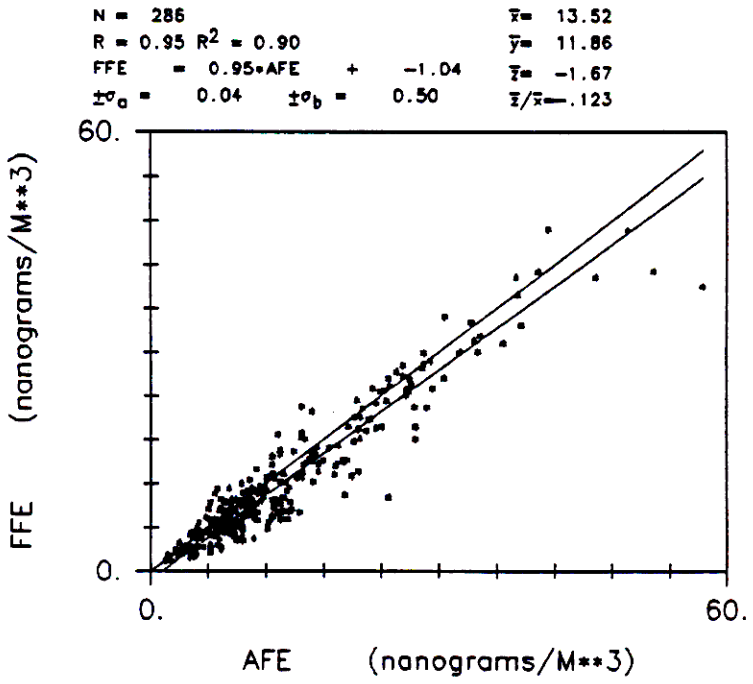

Figure 3C.17: Comparison of iron for A and F modules at Canyonlands, Hopi Point, Bullfrog, and Page.

Since the calibration protocol is similar to that for the IMPROVE sampler, we can assume that the uncertainty in the volume is also 3% for the DRUM sampler.

Estimated Precision and Accuracy of Sizing

The comparison between theory and experiment for the collection efficiency of the configuration used at WHITEX is shown below in Figure 3C.30. The new computer code of Raabe[9] not only matched DRUM size calibration data with monodispersed aerosols, it also explained the published experimental data for the Low Pressure Impactor.[10] The measurements of flow rate indicate that the size cuts were close to the defined values.

Laboratory tests of accumulation mode particles indicate that losses during sampling are (10.7%±1.2%) for polydispersed aerosols. Visual analysis of the orifices indicates that this loss is evenly distributed among stages 5 to 8. This loss was not included in the data base, but was incorporated in the comparisons with filter data.

Measurements taken during low humidity indicate that there is negligible particle bounce-off from stage to stage.[11] These measurements showed that the stage 1 concentrations were 5000 times those on stage 6, a result not possible if bounce-off occurred.

Estimated Precision and Accuracy of Analysis

The DRUM sampler strips were analyzed by two PIXE detectors centered on the 2 *mm* x 4.2 *mm* spot on each strip. The 2 *mm* width was equal to 6 hours for the WHITEX rotation rate, and it was accurate to ±20 minutes for time width. The exact time of analysis was verified by knowing

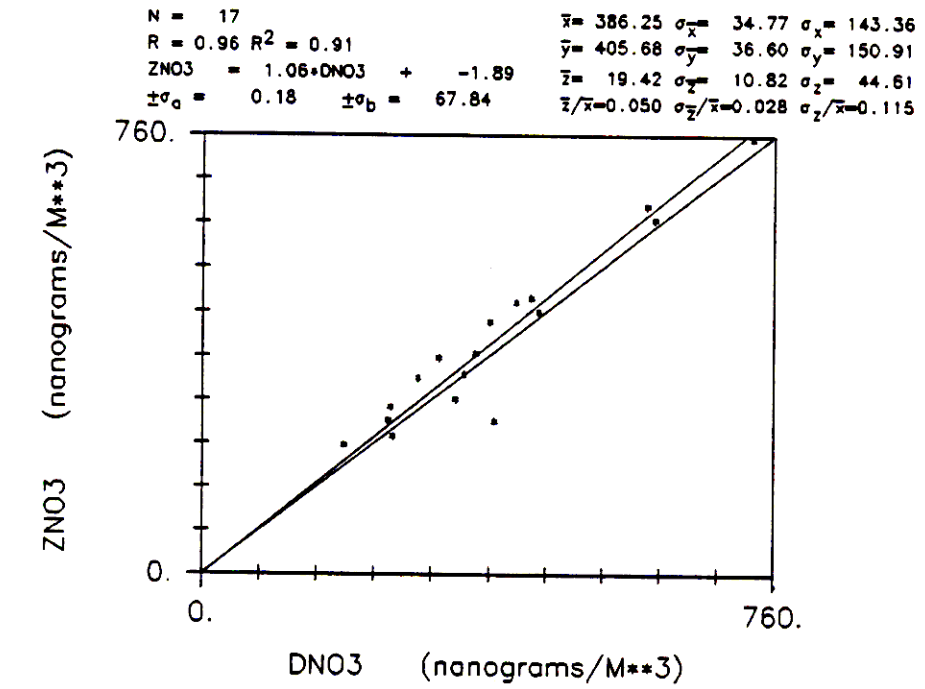

Figure 3C.18: Comparison of total nitrate on special module and nitrate on normal module at Canyonlands.

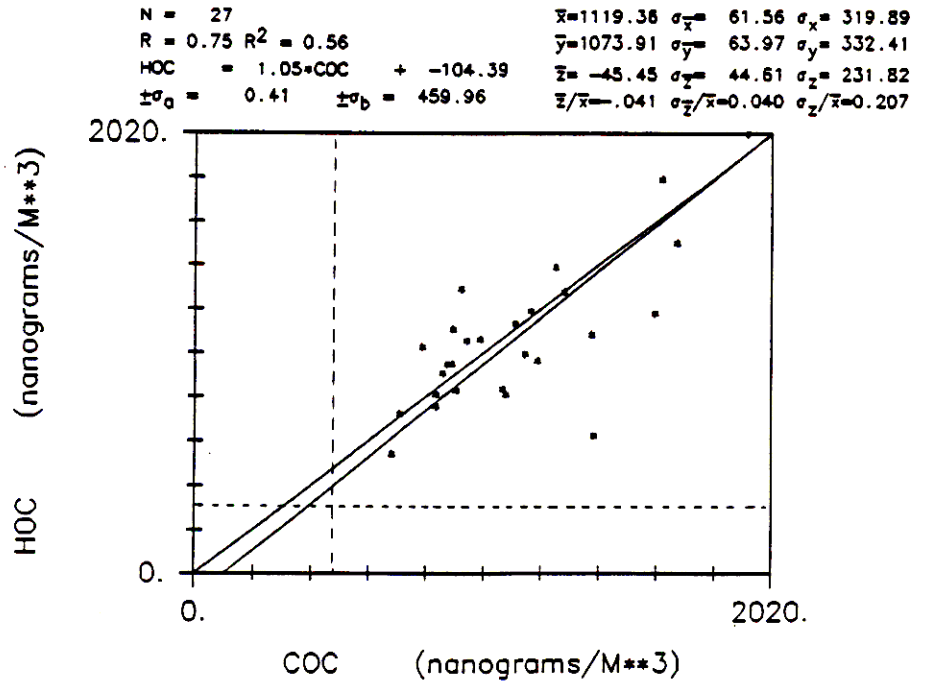

Figure 3C.19: Comparison of organic carbon on special module and on normal module at Page.

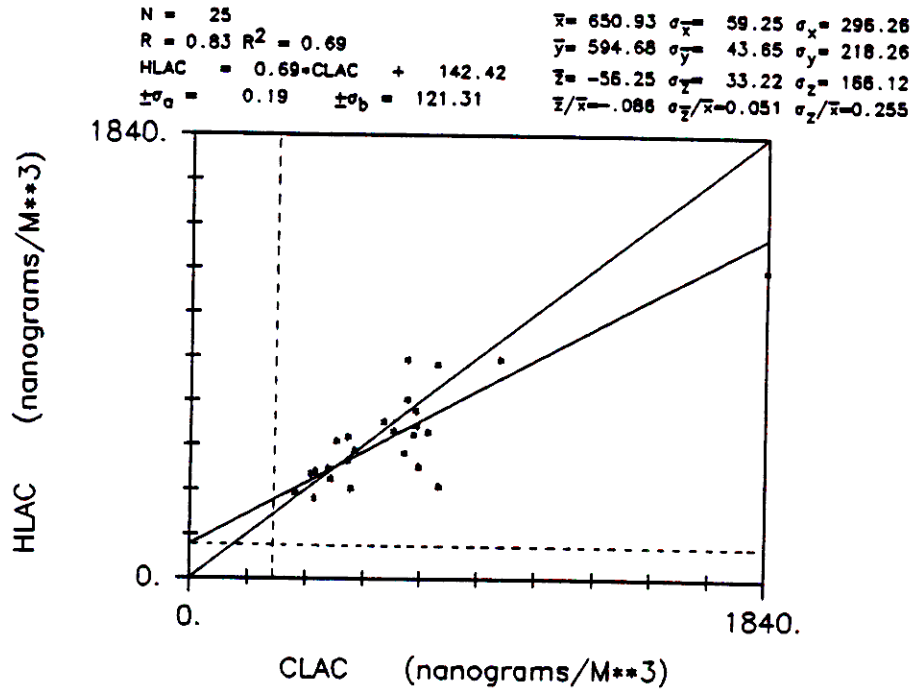

Figure 3C.20: Comparison of light-absorbing carbon on special module and light-absorbing carbon on normal module at Page.

the duration of the sampling and the length of deposit. Unfortunately, the rotation rate was off by 4 minutes (out of 6 hours) and the error promulgated. This required computer averaging of the data to match the filter samples, which in turn increased uncertainties.

The system was calibrated using thin elemental standards from Micromatter Corp., and included the foils $NaCl$, CuS, Al, CaF, Pb, Mo, and Ti. Other elements were calibrated by interpolation on a logarithmic plot. The two detectors overlapped elements near iron: PIXE 1 $Na \rightarrow Zn$; PIXE 2 $Mn \rightarrow Pb$. The iron peak in PIXE 1 agreed with that in PIXE 2 to about ±5%, and total estimated error was set at ±8%. This is higher than for the filters due to the generally very light loadings on the DRUM strips.

Minimum Detectable Limits

Minimum detectable limits were calculated in the same manner as for PIXE with filters. Typically there were a few ng/m^3 in the range of iron, and about 10 ng/m^3 near S and Pb.

Overall Precision and Accuracy

The combination of sampling and analytical error for the DRUM sampler yielded uncertainties of ±12% for a given size regime. These values could be compared to filters taken side by side, if one compares a <2.5 μm filter to DRUM stages 4, 5, 6, 7, 8, and the afterfilter. However, the propagation of errors yielded a typical increase in the compared values of $f2 \times \sigma_{strip}$, or ±17%.